Bioorganic & Medicinal Chemistry 20 (2012) 4838–4847

Contents lists available at SciVerse ScienceDirect

Bioorganic & Medicinal Chemistry

journal homepage: www.elsevier.com/locate/bmc

Experimental and 'in silico' analysis of the effect of pH on HIV-1 protease inhibitor affinity: Implications for the charge state of the protein ionogenic groups

José L. Domínguez [a], Thomas Gossas [b,†], M. Carmen Villaverde [a], U. Helena Danielson [b,*], Fredy Sussman [a,*]

[a] Departamento de Química Orgánica, Facultad de Química, Universidad de Santiago de Compostela, 15782 Santiago de Compostela, Spain
[b] Department of Chemistry, Uppsala University, Uppsala, Sweden

ARTICLE INFO

Article history:
Received 14 February 2012
Revised 21 May 2012
Accepted 25 May 2012
Available online 7 June 2012

Keywords:
pH effect
Ligand binding affinity
HIV-1 PR
Surface plasmon resonance
Molecular mechanics
Ionizable residues
Protonation states
Asp catalytic dyad

ABSTRACT

The pH dependence of the HIV-1 protease inhibitor affinity was studied by determining the interaction kinetics of a series of inhibitors at three pH values by surface plasmon resonance (SPR) biosensor analysis. The results were rationalized by molecular mechanics based protocols that have as a starting point the structures of the HIV-1 protease inhibitor complexes differing in the protonation states as predicted by our calculations. The SPR experiments indicate a variety of binding affinity pH dependencies which are rather well reproduced by our simulations. Moreover, our calculations are able to pinpoint the possible changes in the charged state of the protein binding site and of the inhibitor that underlie the observed effects of the pH on binding affinity. The combination of SPR and molecular mechanics calculations has afforded novel insights into the pH dependence of inhibitor interactions with their target. This work raises the possibility of designing inhibitors with different pH binding affinity profiles to the ones described here.

1. Introduction

The affinity of a ligand for a protein is dependent on environmental conditions, such as ionic concentration and pH, which influence inhibitor protein interactions not only on a biochemical, but also at a cellular level.[1] For this reason, the dependence of inhibitor binding on pH could have important implications for drug discovery. To study this issue, we use the protease of the human immunodeficiency virus 1 (HIV-1 PR), as a benchmark. This enzyme is a very successful AIDS therapeutic target, because its inhibition precludes the proteolytic cleavage of viral protein precursors into functional units, and hence viral replication. In the process, the HIV-1 PR has turned into the most studied member of the aspartic protease family.[2,3]

Usually, the inhibitor binding affinity to HIV-1 PR is determined in assays performed at the optimum enzymatic pH (ca. 5.5), where the enzyme is catalytically active. However, it is possible that HIV-1 PR inhibitors may bind also at physiological pH if they are to be useful as drugs, as has been suggested for BACE-1 inhibitors.[1] In fact many HIV-1 PR inhibitors are less active in cell and animal assays than in the low pH tests used to screen the leads. Nevertheless, there are very few studies dealing with the pH dependence of the binding affinity.[4–6] The emergence of surface plasmon resonance (SPR) has open new venues for this endeavor since it avoids the ambiguities and problems of the FRET based techniques,[1,7,8] precluding the need for a protocol based on a competitive regime with a substrate, whose binding and catalysis may be pH dependent. Members of our group have already used SPR techniques to study different aspects of inhibitor binding to HIV-1 PR. In this line of work we found that interaction kinetics rate constants rather than inhibition constants can help explain structure activity relationships,[8] and that the inhibitor optimization can be guided by the search of inhibitors with a high association and low dissociation constants.[9]

Abbreviations: HIV-1 PR, human immunodeficiency virus type 1 protease; BACE, β-site APP cleaving enzyme; FRET, fluorescence resonance energy transfer; SPR, surface plasmon resonance; NMR, nuclear magnetic resonance; RU, resonance units; DS, discovery studio; CPIRpK_a, calculation of protein ionization and residue pK_a; DC, dielectric constant; EM, energy minimization; NOE, nuclear Overhauser effect; CHARMM, chemistry at Harvard molecular mechanics; ABNR, adopted basis set Newton Raphson; GBSW, generalized Born with simple switching; LBHB, low barrier hydrogen bond; HB, hydrogen bond.

* Corresponding authors. Tel.: +34 8818 14402.
E-mail addresses: helena.danielson@biorg.uu.se (U. Helena Danielson), fredy.sussman@usc.es (F. Sussman).
† Present address: Beactica AB, Uppsala, Sweden.

0968-0896/$ - see front matter © 2012 Elsevier Ltd. All rights reserved.
http://dx.doi.org/10.1016/j.bmc.2012.05.070

The changes in binding affinity upon a pH change can be traced back to variations in protonation states of the ionogenic groups in the protein residues and inhibitors.

The many studies that have dealt with the protonation state of HIV-1 PR have centered primarily on the Asp dyad (AspA25/AspB25), the catalytic machinery of the enzyme.[4–6,10–12] Some of the studies rely on the pD dependence of the NMR chemical shift of the carboxyl carbons and/or H/D isotope effect upon the Asp carboxyl carbon chemical shift, like the ones used to study the complexes with ligands (KNI-272 and DMP323).[10,11] Recently, high resolution X-ray and neutron diffraction studies on the HIV-1 PR—KNI-272 complex[12] suggest that the dyad is monoprotonated at pH 5.5, in contrast to the diprotonated state predicted by ab-initio quantum molecular dynamics calculations performed earlier on the HIV-1 PR-pepstatin complex.[13] Other studies base their results either partially or totally on molecular mechanics or Poisson Boltzmann calculations.[6]

In this work we address the question of the pH dependence of the binding affinity by evaluating the change in kinetic rate constants (k_{on} and k_{off}) and the dissociation constant K_D, for a group of HIV-1 PR inhibitors of diverse chemical structure, by SPR experiments at three different pH values. The results are rationalized by molecular mechanics calculations that have as a starting point HIV-1 PR structures with the protonation states predicted by a Born approach to the Poisson Boltzmann equation in a molecular mechanics framework. Our results indicate upward pK_a shifts in the Asp dyad values upon binding, a result that was rationalized by the way in which the molecular mechanics calculations represent the existence of low barrier hydrogen bonds between the inhibitor and one of the carboxylate side chains belonging to the Asp dyad.

Our calculations reproduce rather well the binding affinity ranking due to a pH increase and provide a rationale for the experimental results based on the pK_a values of the ionizable groups of the protein and the inhibitor. Furthermore, we predict that the replacement of single atoms or groups of atoms in the inhibitors studied here could lead to ligands with new binding affinity pH dependent profiles.

2. Methods

2.1. SPR biosensor interaction analysis

In order to examine the effect of the pH on the binding affinity we have determined the affinities of a variety of inhibitors at three pH values (4.1, 5.1 and 7.4). An SPR-biosensor instrument (Biacore S51, GE Healthcare, Uppsala, Sweden) was used for the interaction studies. All experiments were carried out at 25 °C and immobilization was performed at a flow rate of 5 μl/min. HIV-1 protease was covalently attached to the carboxymethylated dextran matrix of a CM5 sensor chip (GE Healthcare, Uppsala, Sweden) via primary amines on the protein using standard amine coupling method. A fresh mixture of 0.2 M *N*-ethyl-*N*′-[(dimethylamino)propyl]carbodiimide (EDC) and *N*-hydroxysuccinimide (NHS) was injected for 7 min to activate the carboxyl groups of the dextran matrix. HIV-1 protease (~0.3 mg ml^{-1} in 5 mM maleic acid, pH 6.0) was then injected until sufficient amounts of protein were immobilized (1–2 min). Directly following immobilization, EDC/NHS was again injected for 7 min to stabilize the sensor surface.[14] Ten micromolar Hepes, pH 7.4, 0.15 M NaCl, 3 mM EDTA, 0.005% (v/v) surfactant P-20 (polyoxyethylene sorbatan; GE Healthcare, Uppsala, Sweden) was used as running buffer during the immobilization procedure. The same buffer with addition of 3% DMSO was also used for the interaction studies at pH 7.4. Interaction experiments at acidic pH used acetic acid buffers (10 mM acetic acid, 0.15 M NaCl, at pH 5.1 or 4.1) with addition of 3% DMSO and 0.005% surfactant P-20.

Interaction studies were performed with 3.7–300 nM nelfinavir and 1.2–100 nM saquinavir (generous gifts from Medivir AB, Huddinge, Sweden). Indinavir (Merck Sharp & Dohme Ltd Herts, UK) was used as positive control at 90 nM, to monitor surface activity. The inhibitors were injected in running buffer for 60–120 s at a continuous flow of 90 μl min^{-1}. Dissociation was monitored for 600 s. The sensor surface was regenerated by an injection of 10 μl 1 M LiCl, 50% ethylene glycol at the end of each cycle. Three blank samples were also injected before, in the middle and after each concentration series. A standard solvent correction procedure according to the Biacore S51 methodology handbook (GE Healthcare, Uppsala, Sweden) was included for every experiment.

2.2. SPR interaction data analysis

Binding responses were recorded in resonance units (RU) and presented graphically as a function of time in sensorgrams. Biacore S51 and BIAevaluation software (version 3.0.2, GE Healthcare, Uppsala, Sweden) was used to extract information from the sensorgrams. By subtracting the response from a reference flow cell, and including the solvent correction procedure, signals could be corrected for differences in bulk refractive index and nonspecific binding. An average response of the three blank injections was also subtracted from the sensorgram in order to correct for small systematic distortions arising from differences between the enzyme and the reference surfaces. A 1:1 Langmuir interaction model accounting for limited mass transport[15] was globally fitted to corrected sensorgrams of a series of six different inhibitor concentrations.

2.3. Structure preparation for modeling

The inhibitors studied in this work are listed in Figure 1. They include a variety of chemical motifs that range from those peptidic inhibitors that emerged early in the search for drug leads like Ac-pepstatin up to those that are currently being used clinically in the treatment of AIDS like saquinavir, nelfinavir and indinavir. The relevant pdb entries (1EBW, 1EBY,[16] 5HVP,[17] 1SDV,[18] 2NMW[19] and 3EKX) were downloaded, all hydrogens added and the CHARMM force field[20] atom types and charges assigned. The structure of the complex between HIV-1 PR and inhibitor A008 is not known. We were able to build it from the pdb entry 1AJX by replacing the benzyl groups by 4-hydroxymethylbenzyl moieties and orienting the side chains to avoid strong steric clashes.

2.4. pK_a calculations

The pK_a values for all titratable residues were calculated by the protocol proposed by Spassov and Yan,[21] implemented in Discovery Studio[22] and named calculation of protein ionization and residue pK_a (CPIRpK_a). This protocol, which employs a generalized Born approximation to reproduce solvent effects, allows for the iterative determination of the pK_a of interacting residues. The internal and external dielectric constants (DC) used in these calculations were 10 and 80, respectively, the ionic strength 0.145, and the energy cutoff for clustering was 0.5 kcal/mol. The protocol used here for the prediction of the pK_a value of ionizable residues, applies to all residues of the protein and to the amino acids that form part of the inhibitor. Therefore, this algorithm was able to predict the pK_a values (and the protonation fraction at a given pH) for the acidic amino acids in proteins and for the acidic residues in those inhibitors that have peptidic fragments. Whenever the inhibitors contained ionogenic groups (like the amino groups in nelfinavir, indinavir and saquinavir, or the statin moiety carboxylate group in Ac-pepstatin), the pK_a values were evaluated for both charge states of the inhibitor.

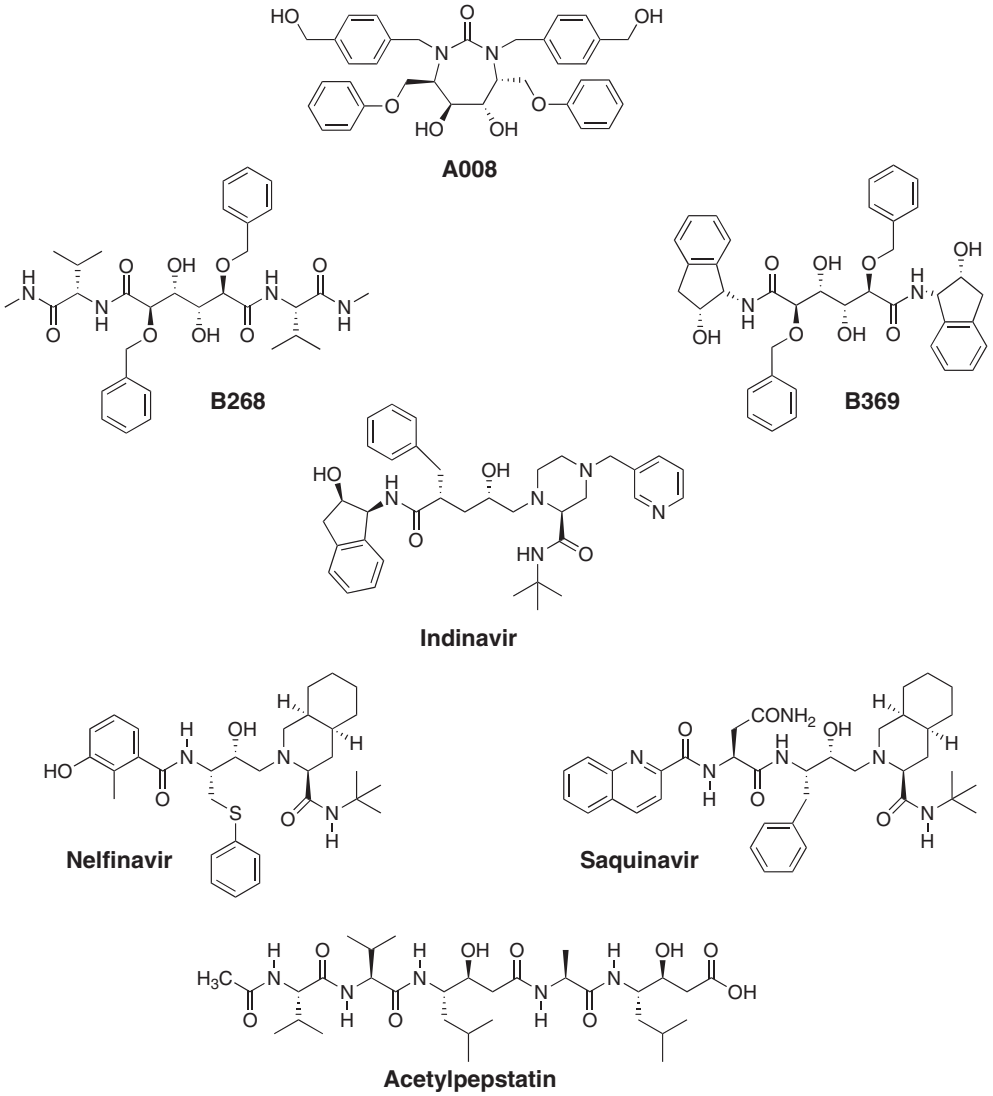

Figure 1. Inhibitors studied in this work.

Since the module CPIRpK_a does not evaluate the pK_a values of the inhibitors ionogenic groups, we have used the pK_a values calculated in solution by the Epik module[23] implemented in the Schrödinger suite of programs.[24]

2.5. Affinity predictions

For our affinity calculations we chose the protonation states predicted as the prevalent ones at pH 4.1, 5.1 and 7.4 on the basis of the calculated protonation fraction for each residue by the pK_a predictor DS module. Whenever the pH fell very close to the pK_a value of a HIV-1 PR acidic residue, additional structures with the alternative protonation states are needed in order to evaluate our scoring function (see below). Given the large number of initial structures to study, we choose a simplified method for treating them, based on a multi-step molecular mechanics energy minimization (EM) protocol. The first part incorporated two EM protocols devoted to optimize the proton position and the hydrogen bond ligand–protein network observed in the crystallographic structure. In the first EM we fixed all heavy atoms, while in the second we placed NOE constraints on the heavy atoms that participate as donors and acceptors in hydrogen bonds between the ligand and the protein. Each of the EM had two segments: the first one was an EM steepest descent segment of 2000 steps, and the second one a stage of 50,000 steps with an ABNR optimization protocol. The tolerance gradient in all these calculations was 0.001 kcal/mol Å^2. For all the EM calculations we used an implicit solvation term based on the generalized Born approach with simple switching (GBSW),[25] with protein dielectric constant of 5. This value was chosen to take into account implicitly the protein flexibility.[6]

For each of the optimized structures we obtained the binding affinity scoring function using the following expression:

$$\Delta G_{\text{bind}} = \Delta G_{\text{mm}}(\text{P:L}) - \Delta G_{\text{mm}}(\text{P}) - \Delta G_{\text{mm}}(\text{L}) + \Delta G_{\text{gb}}(\text{P:L}) - \Delta G_{\text{gb}}(\text{P}) - \Delta G_{\text{gb}}(\text{L}) \quad (1)$$

where ΔG_{mm} and ΔG_{gb} indicate the molecular mechanics CHARMM force-field[20] and the GBSW solvation[25] components, respectively, for the protein–ligand complex (P:L), protein (P) and ligand (L).

All the EM and analysis calculations were performed with the CHARMM suite of programs[26] in the 2400 processors Finisterrae supercomputer facility available at the supercomputing center of Galicia (CESGA).

As mentioned above, there exists the possibility that for a given acidic residue, both the charged and neutral protonation states would be highly populated. In that case, the final binding scoring

function was obtained through a weighted binding scoring function for both protonation states.

$$\Delta G_{bind} = X_1 \Delta G_{bind}(0) + (1 - X_1)\Delta G_{bind}(-1) \quad (2)$$

Where $\Delta G_{bind}(0)$ and $\Delta G_{bind}(-1)$ are the scoring function values when an acidic residue is protonated or charged, respectively. X_1 is the protonation fraction for a specific residue, obtained from its pK_a value through the Henderson-Hasselbalch equation for a given pH.

2.6. Effect of the dielectric constant on binding affinities

It is known that the dielectric constant has a strong effect on the calculated pK_a values of the ionogenic groups.[6] In order to evaluate the effect of this parameter on our results, we re-evaluated the pK_a values of the titratable residues for some of the complexes studied at various dielectric constants ranging from the default value of 10 up to a final value of 20. As before, once the charge states of these complexes were estimated (see Section 2.4), the binding affinities for the complexes studied were obtained using the protocols described in Section 2.5 with the new higher value of DC.

3. Results

3.1. Kinetic analysis and pH dependencies of inhibitor interactions

The interaction kinetic parameters for saquinavir and nelfinavir were determined at three different pH values (4.1, 5.1 and 7.4) (see Table 1). The pH dependencies of the complete series of HIV-1 PR inhibitors analyzed in this study is shown in Figure 2. The binding affinity patterns upon a pH change differ greatly for dissimilar inhibitors, as it has been reported earlier.[7] The new data for nelfinavir and saquinavir show that these inhibitors have similar pH dependencies, but that the kinetics are shifted, with saquinavir having 10-fold slower dissociation rates and slightly faster association rates, resulting in higher affinities at all pH values.

In order to rationalize these experimental data, we calculated the protonation states of the HIV-1 PR—inhibitor complexes at the 3 pH values utilized in our SPR experiments, and then used them to predict the binding affinity ranking due to a pH increase. These results are presented below and discussed in a separate section.

3.2. Prediction of pK_a values for protein residues

3.2.1. Validation of the pK_a prediction method

NMR has been the main tool for experimental determination of the protonation state of the titratable residues in HIV-1 PR complexes. The most extensive NMR studies have been carried out on the HIV-1 PR bound to DMP323, a cyclic urea inhibitor.[11] In order to test our pK_a predictor protocol we have calculated the pK_a values of the acidic residues in this complex. As shown in Table 2, the protocol used here reproduces rather well the pK_a values for acidic residues for the HIV-1 protease bound to inhibitor DMP323. Many of our calculated trends reproduce those observed experimentally. For instance, our protocol predicts an upward shift in the pK_a value for the residues AspA25/B25 of the catalytic dyad, with respect to the ones that have been determined for a model Asp residue (pK_a 4.1), in agreement with experiment.[11] Moreover, our calculations indicate that the residues Asp A29/B29 become more acidic than the model compound in solution (pK_a 4.1), a trend that is also in agreement with that of the NMR based results.

3.2.2. Effect of the inhibitor on the HIV-1 PR ionizable residues

Some of the inhibitors studied do not have ionizable fragments (see inhibitors A008, A268 and A369) and thus the protein residues pK_a values can be calculated directly (see results in Table 3). Other inhibitors studied here may be neutral or charged at a given pH value, depending on their environment found in the enzyme. Some of them (i.e., indinavir and saquinavir) have more than one amino group that could be protonated over a large range of pH values. Hence it is necessary to have an estimate of the protonation proclivity for all ionizable groups in an inhibitor, ahead of the protein residue pK_a prediction. For this sake, we have carried out the charge assignment based on Epik pK_a predictions for these inhibitors in solution. For instance, indinavir and saquinavir have several amino groups that could be protonated. Our predictions in solution indicate that in saquinavir, the protonated amino group of the quinoline (pK_a <4.0) is much more acidic than the one that belongs to the decahydroquinoline group (pK_a ~10). Hence this latter amino group will be the only one that may stay protonated at all of the pH values used in this work. On the other hand, our pK_a evaluations of indinavir in solution indicate that the amino group that has the higher probability of being protonated in our pH range is one that belongs to the piperazine at the position closest to the pyridine group. In order to shed light onto the effect of ligand charge on the charge state of the protein residues we have calculated the pK_a values for all protein tritratable residues when bound to ionizable inhibitors both in their neutral and charged states. The results are shown in Table 4. Perusal of this table indicate that the charged state of the ionizable residues in the protein will strongly depend on the protonation state of the bound inhibitor for inhibitors with ionogenic groups, an effect specially noticeable for Asp catalytic dyad residues.

3.2.3. Effect of the dielectric constant (DC) on active site charge states

As pointed out earlier, the DC value for the interior of the protein has a strong effect on the resulting pK_a values of the ionizables residues.[6] As shown before by Trylksa et al.[6] raising the DC of the protein interior in the apo and some holo HIV-1 PR systems may result in a decrease of the pK_a values for the HIV-1 PR Asp dyad residues. Hence there is the possibility that an increment in the DC beyond the value of 5 may lead to HIV-1 PR with Asp dyads in the monoprotonated states, in line with some X-ray crystallographic[12] and NMR results.[10]

Table 5 displays the pK_a values for the Asp dyads of some of the complexes studied here as a function of the DC values. Perusal of

Table 1
Interaction kinetic parameters for nelfinavir and saquinavir at pH 4.1, 5.1 and 7.1

Inhibitor	pH	k_{on} (M^{-1} s^{-1})	k_{off} (s^{-1})	K_D (nM)
Nelfinavir	7.4	$8.17 \times 10^5 \pm 7.5 \times 10^3$	$2.8 \times 10^{-3} \pm 3 \times 10^{-5}$	3.40 ± 0.01
	5.1	$3.05 \times 10^6 \pm 4.08 \times 10^5$	$9 \times 10^{-3} \pm 9 \times 10^{-4}$	2.99 ± 0.27
	4.1	$1.66 \times 10^6 \pm 7.73 \times 10^5$	$5.3 \times 10^{-2} \pm 9 \times 10^{-3}$	37.6 ± 13.6
Saquinavir	7.4	$1.02 \times 10^6 \pm 5.0 \times 10^3$	$5.86 \times 10^{-4} \pm 9.5 \times 10^{-5}$	0.577 ± 0.095
	5.1	$4.41 \times 10^6 \pm 5.44 \times 10^5$	$2.73 \times 10^{-3} \pm 2.99 \times 10^{-4}$	0.637 ± 0.153
	4.1	$2.78 \times 10^6 \pm 7.1 \times 10^5$	$1.09 \times 10^{-2} \pm 2.08 \times 10^{-3}$	4.13 ± 0.989

The values for the other inhibitors in this study have been published previously.[7] Errors are given as the standard deviation.

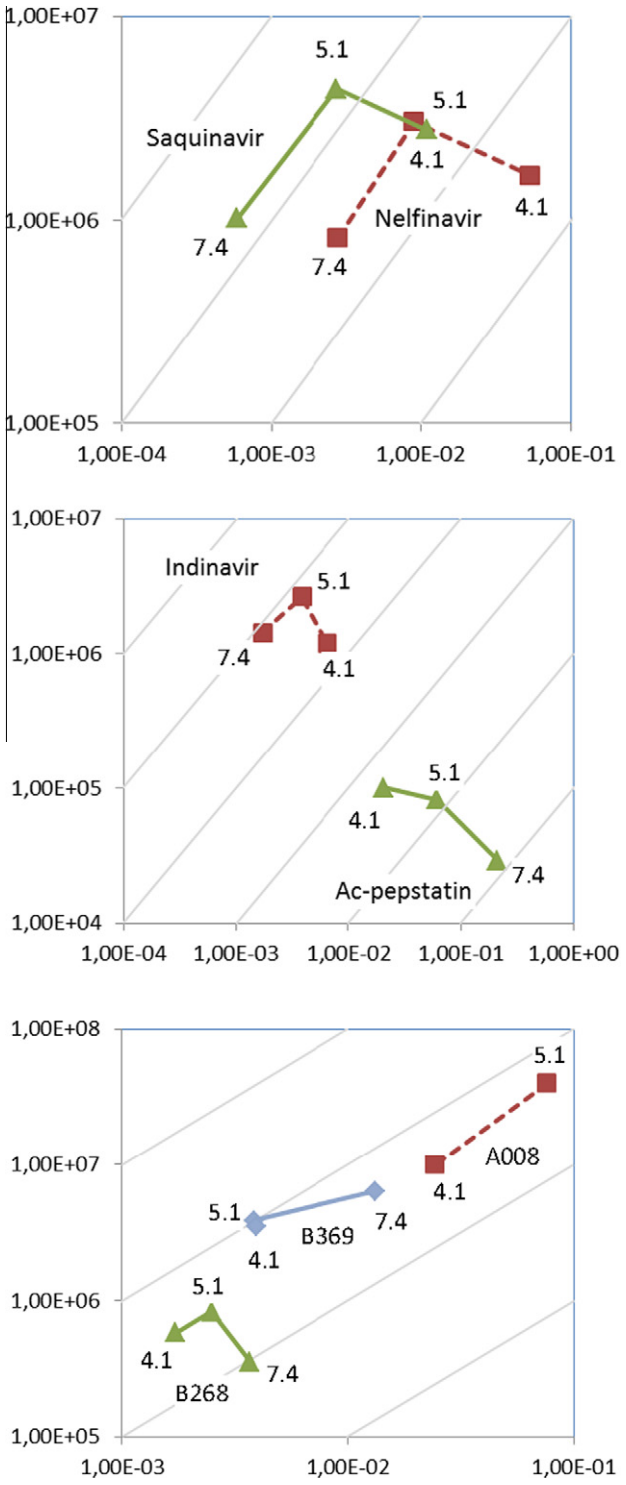

Figure 2. Interaction kinetic plot (k_{on} vs k_{off}) for HIV-1 PR inhibitors at pH 4.1, 5.1 and 7.4. k_{on} and k_{off} units are in M^{-1} s^{-1} and s^{-1}, respectively.

this table indicates that, as expected, increasing the dielectric constant lowers the pK_a values for the Asp dyad residues across the board, irrespective of the chemical structure of the inhibitor. Nevertheless, as we shall see in the next section, the binding affinities calculated with these HIV-1 PR active site charged states do not reproduce as well the affinity trends upon a pH increase as the ones obtained with the lower dielectric constant. (i.e., DC = 5).

Table 2
Comparison of experimental and calculated pK_a values for acidic HIV-1 PR side chains when bound to DMP323

Residue	Calculated	Experimental[a]	
	pK_a	pK_a[b]	pK_a[c]
Asp A25	8.24	8.19	7.7
Asp A29	2.66	2.06	1.97
Asp A30	4.04	3.99	3.96
Asp A60	3.55	3.11	3.15
Asp B25	7.21	8.19	7.7
Asp B29	2.63	2.06	1.97
Asp B30	4.08	3.99	3.96
Asp B60	3.50	3.11	3.15
Glu A21	4.28	4.52	4.48
Glu A34	4.71	4.88	4.91
Glu A35	4.27	3.73	3.75
Glu A65	4.00	3.74	3.72
Glu B21	4.23	4.52	4.48
Glu B34	5.26	4.88	4.91
Glu B35	3.86	3.73	3.75
Glu B65	4.03	3.74	3.72

[a] See Ref. 11 for details.
[b] The experimental pK_a values were determined by fitting the pD dependent chemical shifts using the carboxyl carbon data.
[c] The experimental pK_a values were determined by fitting the pD dependent chemical shifts using the next to carboxyl aliphatic carbon data.

Table 3
Predicted pK_a values for acidic residues when bound to neutral inhibitors

Residue	A008	B268	B369
Asp A25	8.64	10.23	10.24
Asp A29	2.77	3.01	3.51
Asp A30	4.78	4.06	4.08
Asp A60	3.66	3.50	3.60
Asp B25	7.25	6.91	6.70
Asp B29	2.49	3.02	3.84
Asp B30	4.12	3.91	3.69
Asp B60	2.77	3.60	3.47
Glu A21	4.41	4.30	4.25
Glu A34	4.82	5.17	5.23
Glu A35	4.18	4.13	4.15
Glu A65	3.73	3.67	3.65
Glu B21	4.46	4.26	4.26
Glu B34	5.01	5.01	4.98
Glu B35	3.79	3.77	3.95
Glu B65	3.87	3.80	3.77

3.3. Binding affinity pH dependence

3.3.1. Experimental results

Table 6 lists the K_D values obtained by SPR at the three pH values (4.1, 5.1 and 7.4) for all HIV-1 PR—inhibitor complexes studied in this work. The experiments indicate that the HIV-1 PR inhibitors can be classified into three groups, according to the effect of pH on their interaction kinetics and affinities. The first group contains inhibitors that lack any titratable groups (A008, B268 and B369). Although the pH effects on association and dissociation rate constants are different, their affinities are similar at pH 4.1 and 5.1, but lower at 7.4. In the second group formed by Ac-pepstatin, the affinity decreases with increased pH. Finally, the third group of inhibitors (nelfinavir, saquinavir and indinavir) has a similar effect of pH on their interaction kinetics and affinities, with an increase in affinity upon a pH increase from 4.1 to 5.1, but without a further increase when pH becomes neutral (7.4).

3.3.2. Scoring function calculated values

In Table 6 we list also the scoring function values for each inhibitor at the three pH values which allowed us to rationalize the pH

Table 4
Predicted pK_a values for acidic residues when bound to inhibitors with titratable groups

Residue	Indinavir		Nelfinavir		Saquinavir		Ac-pepstatin	
	Charged[a]	Neutral[b]	Charged[a]	Neutral[b]	Charged[a]	Neutral[b]	Charged[a]	Neutral[b]
Asp A25	7.21	7.29	6.15	7.36	5.61	6.56	8.67	8.77
Asp A29	2.19	2.42	2.10	2.23	2.84	2.94	2.79	2.80
Asp A30	3.66	3.76	4.40	4.75	4.29	4.37	4.74	4.75
Asp A60	3.42	3.44	3.09	3.11	3.52	3.53	3.46	3.46
Asp B25	9.41	9.57	8.89	9.85	8.03	8.74	7.30	7.41
Asp B29	3.35	3.51	2.11	2.32	2.31	2.52	2.37	3.30
Asp B30	4.56	4.60	3.94	4.08	4.02	4.15	3.88	5.04
Asp B60	3.36	3.37	3.24	3.25	3.01	3.03	3.69	3.72
Glu A21	4.26	4.29	4.38	4.41	4.62	4.63	4.81	4.83
Glu A34	4.32	4.35	4.98	5.05	5.02	5.41	5.31	5.35
Glu A35	4.23	4.25	3.68	3.71	3.74	3.76	4.14	4.15
Glu A65	3.67	3.67	3.58	3.60	3.54	3.55	4.09	4.09
Glu B21	4.47	4.52	4.53	4.55	4.09	4.12	4.95	4.95
Glu B34	4.72	4.83	5.07	5.11	5.20	5.25	4.85	4.86
Glu B35	3.65	3.68	3.97	4.00	4.23	4.25	3.72	3.74
Glu B65	3.83	3.85	3.56	3.57	3.75	3.76	3.46	3.47

[a] Inhibitor in the singly charged state.
[b] Inhibitor in the neutral state.

Table 5
Predicted catalytic dyad pK_a values dependence on the protein dielectric constant

Inhibitor	Catalytic dyad	Protein dielectric constant[a]			
		10	12	15	18/20
A008	Asp A25	8.64	7.74	6.70	6.47
	Asp B25	7.25	6.66	5.93	4.77
B268	Asp A25	10.23	8.86	7.67	6.87
	Asp B25	6.91	6.20	5.50	5.02
B369	Asp A25	10.24	8.96	7.76	6.53
	Asp B25	6.70	6.01	5.32	4.60
Saquinavir	Asp A25	5.61(6.56)	—	—	4.07(4.83)
	Asp B25	8.03(8.74)	—	—	5.63(6.14)

[a] Numbers in parenthesis correspond to those obtained with the neutral inhibitor.

binding ranking based on the charge state of the ligands and protein residues (see discussion).

As pointed out above, increased DC values lead to monoprotonated Asp dyads at the enzyme optimal pH for many HIV-1 PR—ligand complexes, in line with some NMR and neutron diffraction results. Hence, in order to explore the effect of this variable, we calculated the binding affinity for charge distributions at higher DC value. Table 7 displays scoring function affinities for Ac-pepstatin and nelfinavir at DC 18. As seen from this Table affinity prediction calculations for instance for nelfinavir fare worse than those presented in Table 6. This outcome supports to some extent the charge state of the ionizable residues used for the calculations presented in Table 6, at a lower DC value.

4. Discussion

4.1. Effect of the inhibitor on the pK_a of the HIV-1 PR ionizable residues

Perusal of Tables 3 and 4 shows that the chemical structure and charge state of the inhibitors have a profound influence on the pK_a values of the side chains of titratable residues. Nevertheless, there are some commonalities amongst the protein residues pK_a trends. For instance, our calculations indicate that the largest pK_a shifts, with respect to the values of model compounds in solution, are for the acidic residues that lie in the inhibitor binding pockets, especially those that reside in S1/S1′ (e.g., those that belong to the Asp dyad). These latter residues vary their pK_a values by several units upon change of inhibitor. By comparison, the other acidic res-

Table 6
Effect of pH on experimental and calculated affinity value

Inhibitor	Scoring function (kcal/mol)[a]			K_D (nM)[d]		
	pH 4.1[b]	pH 5.1	pH 7.4[c]	pH 4.1	pH 5.1	pH 7.4
A008	−79.85 (−**79.98**)	−**80.18**	−**78.75**	1.83	1.84	6.95
B268	−**87.22**	−**87.46**	−**85.50**	2.97	3.00	10.80
B369	−99.93 (−**101.35**)	−**101.42**	−**99.69**	1.14	1.00	13.90
Indinavir			−100.76 (−**92.82**)	5.45	1.38	1.20
Indinavir (+)	−**88.55**	−**91.96**	(−92.82)			
Nelfinavir		−**91.5**	−90.70 (−**90.80**)	37.6	2.99	3.40
Nelfinavir (+)	−**88.55**	−89.12	−92.80			
Saquinavir		−**92.38**	−**96.23**	4.13	0.637	0.577
Saquinavir(+)	−**91.44**	−92.49	−94.89			
Acpepst	−**95.73**	−88.80	−94.2 (−95.0)	208	759	8150
Acpepst (−)	—	−**92.17**	−**91.84**			

[a] Thick numbers indicate the protonation states that have similar trends to the experimental.
[b] Values in parentheses were calculated by weighting the affinities obtained by taking into account both protonation states for the residue Asp 30.
[c] Values in parentheses were calculated by weighting the affinities obtained by taking into account both protonation states for the residue Asp 25.
[d] Data from Table 1 (nelfinavir and saquinavir) and Ref. 7.

Table 7
Calculated binding affinity scoring funtion values in kcal/mol at DC 18

Inhibitor		pH value		
		4.1	5.1	7.4
Nelfinavir	Charged	−98.81	−97.95	−96.93
	Neutral	−96.73	−96.84	−94.13
Ac-pepstatin	Charged	−108.59	−108.47	−104.62
	Neutral	−109.02	−104.29	−102.93

idues that reside in S2/S2′ and S3/S3′ pockets display smaller but noticeable changes, like for instance the downward pK_a shift in AspB30 when bound to the charged Ac-pepstatin. This trend can be traced back to the binding site structure (see Fig. 3), which shows that this residue is part of an intricate microenvironment, making polar interactions with the C-terminal carboxylate of the inhibitor and with the side chain of Lys B45. The overall predicted shifts for all acidic residues follow similar trends to the ones observed in NMR experiments for the HIV-1 PR—DMP323 complex.[11]

On the other hand, NMR based protonation state assignment for the Asp dyad when HIV-1 PR is bound to pepstatin A[27], are at variance with our predictions for the Asp dyad when the enzyme is bound to Ac-pepstatin. Our results indicate that the Asp dyad will only be in the monoprotonated state at the highest pH (7.4), while the NMR results support a single charged Asp dyad over a wider range of pH values. The experimental support for the monoprotonated state was obtained from the analysis of ^{13}C NMR data, which exhibits two distinct signals at 172.4 and 178.8 ppm that remain unchanged in the pH range between 2.5 and 6.5, thus indicating that the Asp dyad protonation state does not change in this pH range. Of the two peaks, the one at low field is the only one that undergoes an isotopic shift.[27] Nevertheless, these NMR results seem to be amenable to more than one interpretation. Piana et al.[13] proposed a diprotonated Asp dyad based on an ab-initio molecular dynamics assignment that includes the calculation of ^{13}C chemical shifts and isotopic shifts. In their work, they show that the only Asp dyad charged state that reproduces these NMR observables is the neutral one, in agreement with our predictions. For other inhibitors, like KNI-272, recent results of a high resolution X-ray structure, together with a neutron diffraction study[12] display the existence of electron density only next to the oxygen of one of the Asp residues in the Asp dyad, supporting the existence of a monoprotonated assignment for this system.

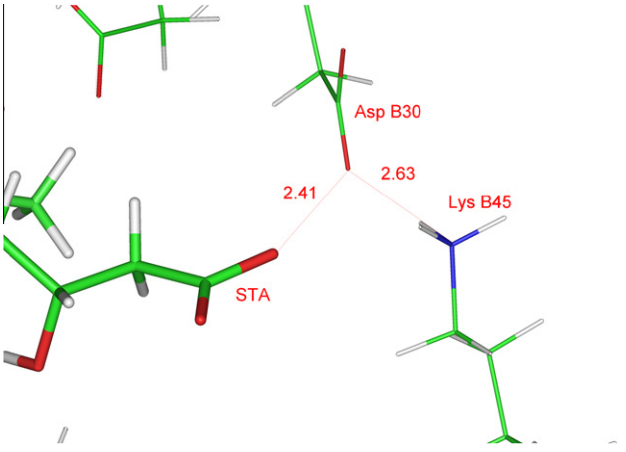

Figure 3. Microenvironment of the Asp B30 residue when bound to acetylpepstatin. Notice the closeness of the C-terminal carboxylate of the statine residue (STA) of the inhibitor with the side chains of Asp B30 and Lys B45. Distances are in Å.

The results shown here suggest that the Asp dyad charge state is neutral at the pH value at which the enzyme is most active (i.e., 5–6), since the pK_a values of their Asp residues are for the most part above six. The results listed in Tables 3 and 4 predict that the Asp dyad monoprotonated state is only prevalent at the highest pH value (7.4) when HIV-1 PR is bound to inhibitors B268, B369, indinavir, nelfinavir and saquinavir. As seen from these tables, the complex where the Asp dyad becomes monoprotonated at the lowest pH (5.6) is the one formed with saquinavir, when this ligand is protonated.

We propose a possible explanation for this result based on the existence of a low barrier hydrogen bond (LBHB) between a hydroxyl group located on the inhibitor's isostere and the oxygen of a carboxylate group that belongs to the Asp dyad (See below). One of the defining characteriztics for a LBHB is the existence of a very short hydrogen bond distance between donor and acceptor.[28] Already, in some of the earliest crystallographic structures of HIV-1 PR complexes (eg., HIV-1 PR bound to Ac-pepstatin) it was observed that the distance from the hydroxyl oxygen of the inhibitor to one of the oxygens of the side chain of an Asp dyad member could be as short as 2.2 Å,[17] raising the possibility of a LBHB between these two atoms.

The existence of compact hydrogen bonds (HB's), that provide support for LBHB's, have been confirmed by the X-ray and neutron diffraction studies of ligand bound aspartic proteases, like in endothiapepsin,[29] and in BACE-1 bound to peptidic inhibitors,[30] suggesting that LBHB's may be a common feature for some aspartic protease-inhibitor complexes. It has been posited that in LBHB's, the proton that mediates the HB could undergo tunnelling, from the energy-well located next to the hydroxyl oxygen to the one next to the carboxylate oxygen.[28] In such a system the proton could be found at both positions (see Fig. 4, panel B), resulting in the dispersion of the negative charge of the Asp residue. It may be argued that the tunnelling in the LBHB populates the Asp dyad diprotonated state, and hence it may be claimed that this charged state could be a molecular mechanics compromise representation of the entities implied by LBHB (Fig. 4).

Finally, the results presented in Tables 3 and 4 indicate that the protonation states of the HIV-1 PR titratable residues will depend strongly on the chemical structure and ionization state of each inhibitor, a similar result to that obtained recently by us on BACE-1, another member of the aspartic protease family which has become an Alzheimer's disease drug target.[1]

4.2. Binding affinity pH dependence

Table 6 lists the experimental as well as the inhibitor affinities predicted by our scoring function. There are two issues that are crucial for comparing the calculated affinities to the experimental ones. The first one relates to the fact that in some cases the pK_a values of some of the acidic residues present in the active site of HIV-1 PR (e.g., Asp 25, Asp 30) are very close to the pH values used in the evaluation of the binding affinities. In that case these residues could be highly populated both in their neutral and charged protonation states. For instance, as seen from Table 3, when HIV-1 PR is bound to inhibitor B369, the calculated pK_a value for residue Asp A30 is 4.08, leading to almost equal populations of ionized and neutral charged states for this residue at pH 4.1. Another example relates to the Asp dyad residues, which exhibits large pK_a shifts to values that are more typical for basic residues. In some cases (indinavir, nelfinavir) their pK_a values are close to the highest pH value studied (7.4), resulting also in similar populations at both charged states for the Asp A25 residue. We take into account the existence of multiple protonation states into the binding affinity scoring function Eq. (2) (see methods section), which weights the scoring value function for each possible charged state by their protonation

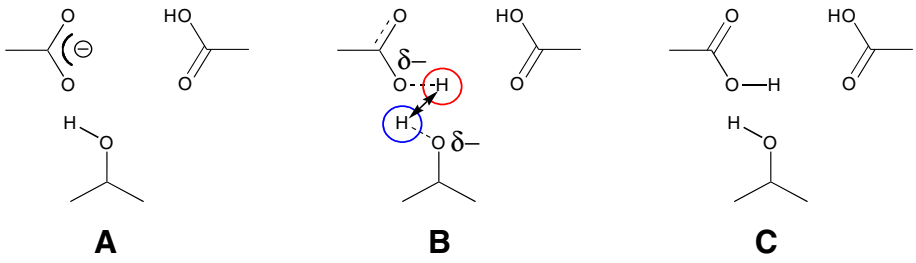

Figure 4. (A) and (C) represent two of the three possible protonation states (mono- and di-protonated) for the Asp dyad, (B) is a schematic representation of a LBHB with the possible proton positions enclosed by red and blue circles.

fractions. Taking into account both charged states in our binding affinity calculation improves in some cases the binding ranking affinity agreement with experimental results. For instance, taking into account the multiple protonation states for Asp A30 increases the binding affinity of B369 for HIV-1 PR at pH 4.1, bringing it closer to that of pH 5.1, in agreement with experiment. Also, as seen from Table 6, taking into account the dual protonation state for Asp A25 ($pK_a = 7.3$) helps to lower the calculated binding affinity, bringing the ranking binding affinity of indinavir at pH 7.4 more in step with experiment.

The other factor that has a strong effect on the binding affinity ranking is the charge state of the inhibitor. As mentioned above, our prediction for the pK_a values of the inhibitors ionizable groups indicate that, nelfinavir, indinavir and saquinavir have each one amino group whose protonated state has a pK_a value above 7, in solution. Nevertheless, perusal of the active site in the ligand–pro-

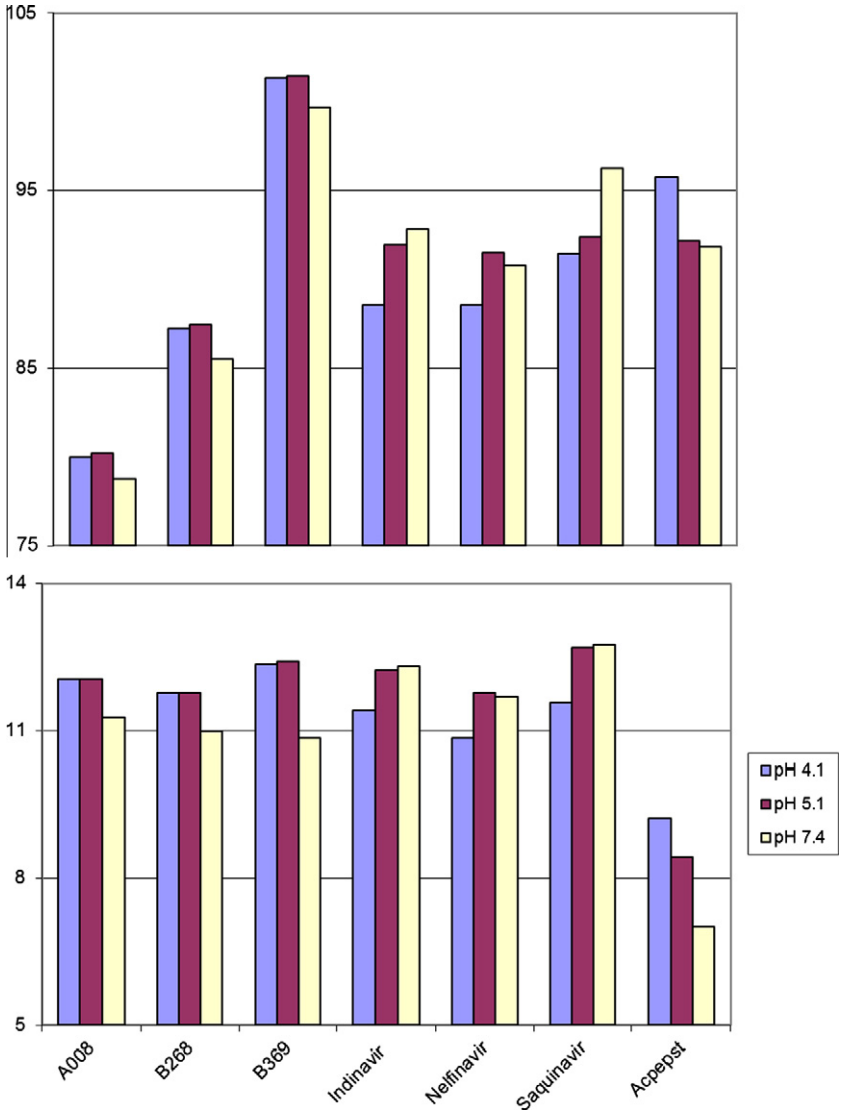

Figure 5. Comparison of the affinity at different pH values obtained by SPR experiments (lower panel) and those obtained from our calculated scoring function in absolute values (upper panel). Values are in kcal/mol.

tein structures indicates that the inhibitors' amino groups do not form hydrogen bonds or ion pairs with any protein polar groups. This raises the possibility that the protonated amino group's pK_a value in these inhibitors would be lower than the ones predicted in solution, leading to a neutral ligand at lower pH value (when bound) than in solution. In order to search for the actual amino group protonation state in these inhibitors we have calculated the scoring function binding affinity for a variety of amino group protonation states, starting with those predicted by the Epik module in the Schrödinger software suite.[24] In the case of nelfinavir, the scoring function results that rank binding affinities better are the result of neutralizing the amino group at pH above or around 5.1. This outcome supports the notion that the pK_a value for the most basic protonated amino group is around this value and suggests a possible explanation for the increase in binding affinity when the pH rises to 5.1. The neutralization of the ligand at pH 5.1 generates a more hydrophobic molecule with a lower desolvation penalty (results not shown), a result that favors binding to the enzyme.

The inhibitor Ac-pepstatin has a carboxylate group in its C-terminal end (see Fig. 1). The Epik calculations in solution predict that this group has a pK_a of 4.4. Hence, if this pK_a is maintained upon binding, this group will be neutral at pH 4.1 and charged at the higher pH values. In order to probe these alternatives we have calculated the protein pK_a values for the two possible inhibitor charge states, prior to the calculation of their binding affinities by our proposed scoring function. As seen from Table 6, our results are in good agreement with the experimental trends, when the above mentioned carboxylate keeps its Epik calculated pK_a value of 4.4. The rationale for this outcome may reside in the polar microenvironment this group is located in (see Fig. 3).

In summary, when both issues (discussed above) that relate to the multiple protonation states of the protein residues and the inhibitor protonation state change at a given pH are taken into account, there is a fair correlation between the observed and calculated binding affinity trends, upon a pH increase. This correlation is better visualized in Figure 5, which graphically display the experimental and observed binding affinity trends.

The results described here raise the possibility of designing inhibitors with different affinity pH dependencies. For instance, we predict that replacement of the C-terminal carboxylate group by a polar non-charged group like an amide may lead to an increase (rather than a decrease) in affinity when the pH rises from 5.1 to 7.4 (see Table 6).

The experimental affinity trends amongst inhibitors, at a given pH value, are not as well reproduced as those related to an increase in pH (see Table 6). This may be related to the conformational entropy penalty contributions from inhibitors that have substantial structural differences. For instance, Ac-pepstatin is predicted to have a higher affinity than A008, in contrast to the experimental trend (see Table 6). Perusal of the chemical structures indicate that the latter inhibitor has a peptidic nature and has many more degrees of freedom than A008 and hence should 'pay' a much higher entropic penalty upon binding to the enzyme. Including the conformational entropic terms should bring the predicted ranking more in line with experiment.

5. Conclusions

In summary, the dependence of the binding affinity to HIV-1 PR on pH was studied by determining the binding affinity of a series of inhibitors at three pH values, by SPR experiments. The results were rationalized by a molecular mechanics based protocol that requires knowledge of the protonation states of all ionizable residues in the HIV-1 PR—inhibitor complexes at the 3 pH values used in this study. Hence, it is of the essence for our calculations to have a robust pK_a predictor. We have validated our algorithm by calculating the pK_a values of all residues in the HIV-1 PR—DMP323 complex and comparing the resulting values with those obtained from NMR experiments. The results indicate that our calculations reproduce rather well the experimental values, validating our pK_a protocol prediction.

Our calculations show that upon inhibitor binding, many ionogenic residues display noticeable shifts from their standard values in solution. The highest pK_a increases are observed for the Asp dyad residues. We hypothesize that LBHB's between one of Asp dyad carboxylate oxygens and a the isotere hydroxyl group are of the essence in rationalizing the Asp dyad protonation states when the HIV-1 PR is in the bound state and bring them in line with some experimental observations.

For the most part, the binding energy differences observed by SPR experiments upon a pH change are rather small. Nonetheless, the calculated trends on binding affinity upon pH increase reproduce with few exceptions the ones observed in the SPR experiments. Our binding affinity predictions support our protein assignments. Moreover, we show that alternative protonation states (that could be present by increasing the protein interior DC) are not able to reproduce the experimental binding affinity trends across the board, a result that lends support to our charge assignment for ionizable residues. On the other hand, the binding affinity trends from one inhibitor to another at a given pH are not well reproduced, since our calculations lack a full evaluation of entropic contributions.

Our calculations support the hypothesis that at a given pH, some acidic residues contribute to the binding affinity to the enzyme through both neutral and charged states. Furthermore, our results also indicate that the inhibitor's titratable groups may have a strong effect on the binding affinity trends by modifying their protonation state upon a pH change. Finally, our studies raise the possibility of designing novel inhibitors with alternative binding affinity pH profiles, which we aim to pursue in further studies.

Acknowledgments

This work was supported by financial aid from the Ministerio de Educación y Ciencia (MEC), Spain and the Xunta of Galicia to M.C.V. and F.S., the Swedish Research Council (VR) to H.D., and a scholarship from the MEC to J.L.D. The Supercomputing Center of Galicia (CESGA) provided computer time.

References and notes

1. Domínguez, J. L.; Christopeit, T.; Villaverde, M. C.; Gossas, T.; Otero, J. M.; Nyström, S.; Baraznenok, V.; Lindström, E.; Danielson, U. H.; Sussman, F. *Biochemistry* **2010**, *49*, 7255.
2. Gosh, A. K. Ed. Aspartic acid proteases as therapeutic targets. Wiley-VCH: Weinheim, 2010. Part Two pp. 107-262.
3. Wlodawer, A.; Vondrasek, J. *Annu. Rev. Biophys. Biomol. Struct.* **1998**, *27*, 249.
4. Velazquez-Campoy, A.; Luque, I.; Todd, M. J.; Milutinovich, M.; Kiso, Y.; Freire, E. *Protein Sci.* **2000**, *9*, 1801.
5. Tripathi, A.; Fornabio, M.; Spyrakis, F.; Mozzarelli, A.; Cozzini, P.; Kellog, G. E. *Chem. Biodiv.* **2007**, *4*, 2564.
6. Trylksa, J.; Antosiewicz, J.; Geller, M.; Hodge, C. N.; Klabe, R. M.; Head, M. S.; Gilson, M. K. *Protein Sci.* **1999**, *8*, 180.
7. Gossas, T.; Danielson, U. H. *J. Mol. Recognit.* **2003**, *16*, 203.
8. Shuman, C. F.; Vrang, L.; Danielson, U. H. *J. Med. Chem.* **2004**, *47*, 5953.
9. Markgren, P.-O.; Schaal, W.; Hämäläinen, M.; Karlén, A.; Hallberg, A.; Samuelsson, B.; Danielson, U. H. *J. Med. Chem.* **2002**, *45*, 5430.
10. Wang, Y.-X.; Freedberg, D. I.; Yamazaki, T.; Wingfield, P. T.; Stahl, S. J.; Kaufman, J. D.; Kiso, Y.; Torchia, D. A. *Biochemistry* **1996**, *35*, 9945.
11. Yamazaki, T.; Nicholson, L. K.; Torchia, D. A.; Wingfield, P.; Stahl, S. J.; Kaufman, J. D.; Eyermann, C. J.; Hodge, C. N.; Lam, P. Y. S.; Ru, Y.; Jadhav, P. K.; Chang, C.-H.; Weber, P. C. *J. Am. Chem. Soc.* **1994**, *116*, 10791.
12. Adachi, M.; Ohhara, T.; Kurihara, K.; Tamada, T.; Honjo, E.; Okazaki, N.; Arai, S.; Shoyama, Y.; Kimura, K.; Matsumura, H.; Sugiyama, S.; Adachi, H.; Takano, K.;

Mori, Y.; Hidaka, K.; Kimura, T.; Hayashi, Y.; Kiso, Y.; Kuroki, R. *Proc. Natl. Acad. Sci. U. S. A.* **2009**, *106*, 4641.
13. Piana, S.; Sebastiani, D.; Carloni, P.; Parrinello, M. *J. Am. Chem. Soc.* **2001**, *123*, 8730.
14. Markgren, P.-O.; Lindgren, M. T.; Gertow, K.; Karlsson, R.; Hämäläinen, M.; Danielson, U. H. *Anal. Biochem.* **2001**, *291*, 207.
15. Karlsson, M.; Pavlov, M. Y.; Malmqvist, M.; Persson, B.; Ehrenberg, M. *Biochemie* **1999**, *81*, 995.
16. Andersson, H. O.; Fridborg, K.; Löwgren, S.; Alterman, M.; Mühlman, A.; Björsne, M.; Garg, N.; Kvarnström, I.; Schaal, W.; Classon, B.; Karlén, A.; Danielsson, U. H.; Ahlsén, G.; Nillroth, U.; Vrang, L.; Öberg, B.; Samuelsson, B.; Hallberg, A.; Unge, T. *Eur. J. Biochem.* **2003**, *270*, 1746.
17. Fitzgerald, P. M. D.; McKeever, B. M.; VanMiddlesworth, J. F.; Springer, J. P.; Heimbach, J. C.; Leu, C.-T.; Herber, W. K.; Dixon, R. A. F.; Darke, P. L. *J. Biol. Chem.* **1990**, *265*, 14209.
18. Mahalingam, B.; Wang, Y.-F.; Boross, P. I.; Tozser, J.; Louis, J. M.; Harrison, R. W.; Weber, I. T. *Eur. J. Biochem.* **2004**, *271*, 1516.
19. Tie, Y.; Kovalevsky, A. Y.; Boross, P.; Wang, Y.-F.; Ghosh, A. K.; Tozser, J.; Harrison, R. W.; Weber, I. T. *Proteins* **2007**, *67*, 232.
20. Momany, F. A.; Klimkowski, V. J.; Schäfer, L. *J. Comput. Chem.* **1990**, *11*, 654.
21. Spassov, V. Z.; Yan, L. *Protein Sci.* **2008**, *17*, 1955.
22. Discovery Studio, version 2.1, Accelrys Inc., San Diego, CA.
23. Shelley, J. C.; Cholleti, A.; Frye, L. L.; Greenwood, J. R.; Timlin, M. R.; Uchimaya, M. *J. Comput. Aided Mol. Des.* **2007**, *21*, 681.
24. Epik, version 2.2, Schrödinger, LLC., New York, NY, 2011.
25. Im, W.; Lee, M. S.; Brooks, C. L., III *J. Comput. Chem.* **2003**, *24*, 1691.
26. Brooks, B. R.; Bruccoleri, R. E.; Olafson, B. D.; States, D. J.; Swaminathan, S.; Karplus, M. *J. Comput. Chem.* **1983**, *4*, 187.
27. Smith, R.; Bereton, I. M.; Chai, R. Y.; Kent, S. B. H. *Nat. Struct. Biol.* **1996**, *3*, 946.
28. Frey, P. A.; Whitt, S. A.; Tobin, J. B. *Science* **1994**, *264*, 1927.
29. Coates, L.; Tuan, H.-F.; Tomanicek, S.; Kovalevsky, A.; Mustyakimov, M.; Erskine, P.; Cooper, J. *J. Am. Chem. Soc.* **2008**, *130*, 7235.
30. Hong, L.; Koelsch, G.; Lin, X.; Wu, S.; Terzyan, S.; Ghosh, A. K.; Zhang, X. C.; Tang, J. *Science* **2000**, *290*, 150.